Simulation of flows at supercritical pressures with a two-fluid code

Markku Hänninen, Joona Kurki
VTT Technical Research Centre of Finland
Tietotie 3, Espoo, P.O. Box 1000, FI-02044 VTT, Finland
markku.hanninen@vtt.fi, joona.kurki@vtt.fi

Abstract

Fossil-fueled power plants have been operated with water at supercritical pressures for decades due to the high thermal efficiency achievable by increasing the system pressure above the critical point. During the recent years, there has been a renewed interest to develop also water-cooled nuclear reactors which work under the supercritical pressure conditions. When such reactor concepts are studied, it is necessary that also the simulation codes used for design and safety-demonstrations of such reactors are able to simulate water flows above the critical pressure. In APROS process simulation software, the two-phase flow can be simulated with a variable level of sophistication: with a homogeneous model, with a 5-equation drift-flux model and with a 6-equation two-fluid model. At supercritical pressures the distinction between the liquid and gas phases disappears: boiling and condensation are not observed, but instead the properties of the fluid vary smoothly from those of a liquid-like fluid to those of a gas-like fluid, and from the macroscopic point of view the supercritical-pressure fluid can always be considered a single-phase fluid. Because of this, the homogeneous model would be ideal for the thermal hydraulic simulation at and above the critical pressure. However, in the nuclear power plant applications the homogeneous model is seldom sufficient for the calculation of two-phase flow below the critical pressure, and thus the six-equation model has to be used in the general case. When the six-equation model is applied to supercritical-pressure calculation, the problems how the model behaves near and above the critical pressure, and how the phase transition through the supercritical-pressure region is handled, are inevitably encountered. Above the critical pressure the heat of evaporation disappears and the whole concept of phase change is no longer meaningful. In the present paper the use of the six-equation thermal-hydraulic model for supercritical-pressure calculation is described. The changes made in the constitutive equations are discussed. The applicability of the numeric model is demonstrated by simulating two basic test cases.

Keywords

Thermal Hydraulics, Supercritical Pressures, System-Code Development

1. INTRODUCTION

The set of constitutive equations needed in the six-equation solution includes friction and heat transfer correlations which are developed separately for both phases. The capability of constitutive equations and the way how they are used has to be carefully examined. One possibility to maintain separate liquid and gas flows in the numeric model is to use a small evaporation heat and apply the concept of the pseudo-critical line. The pseudo-critical line is an extension of the saturation curve to the supercritical pressure region: it starts from the point where the saturation curve ends (the critical point), and it can be thought to approximately divide the supercritical pressure region to sub-regions of pseudo-liquid and pseudo-gas, for at the same point where heat capacity c_p is maximized, the variation of density ρ as function of temperature is also steepest. The thermo physical properties of water/steam undergo rapid changes near the pseudo-critical line and therefore the quality and accuracy of the steam tables is essential in calculation of flows under supercritical conditions. The steam tables used in APROS are based on the IAPWS-IF97 recommendation, which defines the properties of water with a sufficient accuracy over wide range of parameters, including supercritical pressures. The basic work done with testing of new steam and material properties and new correlations implemented in APROS was made earlier [1]. In the present paper the use of the six-equation thermal-hydraulic model for supercritical-pressure calculation is described. The changes made in the constitutive equations are discussed. The applicability of the numeric model is demonstrated by simulating an instant emptying of a horizontal pipe. Several cases with different initial conditions are calculated and discussed. The calculation of the wall-to-fluid heat transfer is examined with a model of supercritical water flowing through an electrically heated pipe.

2. SIMULATION OF FLOWS WITH THE TWO-FLUID MODEL

2.1. Principles of the six-equation solution

The six-equation solution of the APROS code is based on the one-dimensional conservation laws of mass, momentum and energy. When these laws are applied for both the liquid and gas phases, all together six partial differential equations are obtained. These equations can be written in the form

$$\frac{\partial(\alpha_k \rho_k)}{\partial t} + \frac{\partial(\alpha_k \rho_k u_k)}{\partial z} = \Gamma_k \tag{1}$$

$$\frac{\partial(\alpha_k \rho_k u_k)}{\partial t} + \frac{\partial(\alpha_k \rho_k u_k^2)}{\partial z} = \Gamma_k u_{ik} + \alpha_k \rho_k \vec{g} + F_{wk} + F_{ik} \tag{2}$$

$$\frac{\partial(\alpha_k \rho_k h_k)}{\partial t} + \frac{\partial(\alpha_k \rho_k u_k h_k)}{\partial z} = \alpha_k \frac{\partial p}{\partial t} + \Gamma_k h_{ik} + q_{ik} + q_{wk} + F_{ik} u_{ik} \tag{3}$$

In the equations the subscript k is either l for the liquid phase or g for the gas phase, the subscript i refers to the interface between the phases, and the subscript w to the wall of the flow channel. $\Gamma_g = -\Gamma_l$ is the mass evaporation rate, F the friction force and q the heat transfer rate. In the energy equation (3) the term h is the *total solved enthalpy*, i.e. static enthalpy plus the kinetic energy per unit mass, $h_{kin} = ½v^2$ where v is the flow

velocity. The potential energy due to gravity is considered small and has been omitted in the energy equation.

The phenomena which depend on the transverse gradients, like friction and heat transfer between the gas and liquid phases and between the wall and both the phases, have been described with empirical correlations. The correlations are strongly dependent on the flow regime and thus usually different correlations have to be used for different flow regimes. The flow regimes which are treated in the code are *bubbly*, *annular*, *droplet* and *stratified* flows. In the calculations, the real prevailing flow mode usually consists of more than one individual flow regime. When the correlations are applied, the different flow regimes are taken into account by weighting factors.

In the supercritical pressure conditions the phenomena related to two phase concept disappear. Therefore the correlations used for two-phase heat transfer and friction must be considered when the conditions change from subcritical pressure two-phase area to supercritical pressure area. In the following the interfacial heat transfer and wall heat transfer as well as the interfacial friction and wall friction are discussed in detail.

2.2. Calculation of interfacial heat and mass transfer

In two-phase flow the heat and mass transfer between liquid and gas has to be calculated. The calculation of interfacial mass transfer is based on the requirement that the energy balance over the interface is zero. When it is assumed that the interface is at saturated state the following relationship is obtained

$$\Gamma_i = -\frac{q_{\mathrm{i1,i}} + q_{\mathrm{ig,i}} - q_{\mathrm{wi}}}{h_{\mathrm{g,sat}} - h_{\mathrm{1,sat}}} \tag{4}$$

where q_{wi} is the heat flowing from the wall directly to the interface. The interfacial heat transfer rates are calculated separately for liquid and gas side.

From liquid side the heat transfer is

$$q_{\mathrm{i1},i} = -K_{\mathrm{i1},i}\left(h_{\mathrm{1,stat}} - h_{\mathrm{1,sat}}\right) \tag{5}$$

From gas side the interface heat transfer is

$$q_{\mathrm{ig},i} = -K_{\mathrm{ig},i}\left(h_{\mathrm{g,stat}} - h_{\mathrm{g,sat}}\right) \tag{6}$$

Depending on the heat flows the mass transfer is either positive (evaporation) or negative (condensation). The interfacial heat transfer coefficients depend strongly on the void fraction and on the phase flow velocities.

When the critical pressure is approached from lower pressure side the evaporation heat is gradually disappearing. Actually the decreasing rate of the evaporation heat is accelerating near the critical point as it can be seen in Figure 1.

Because the present two-fluid model treats the supercritical fluid as a two-component

mixture, the formalism of interfacial heat and mass transfer has to be extended to the supercritical pressure regime. The objective of this extension is to treat the fluid as liquid when its enthalpy is below the pseudo-critical enthalpy and as gas when its enthalpy is above the pseudo-critical enthalpy. Additionally it is desirable that the pseudo phase transition occurs as fast as possible so as to minimize the time the pseudo void fraction is not strictly zero or unity, but without introducing any numerical instabilities to the solution.

In the present model the latent heat of vaporization is set to a constant value L_{pe} at the supercritical pressure region, and the pseudo-saturation enthalpies are then set to to

$$\begin{aligned} h_{\mathrm{l,sat}}(p) &= h_{\mathrm{pc}}(p) - \frac{L_{\mathrm{pe}}}{2} \\ h_{\mathrm{g,sat}}(p) &= h_{\mathrm{pc}}(p) + \frac{L_{\mathrm{pe}}}{2} \end{aligned} \tag{7}$$

With these definitions, the interfacial heat and mass transfer can be calculated identically to the approach used at subcritical pressures.

Because the interfacial heat transfer coefficients, which at the two-phase region are normally calculated using suitable correlations, have no physical relevance, they can be chosen arbitrarily to yield the desired effect. In APROS, the interfacial heat transfer coefficients at supercritical pressures are calculated starting from a shape function

$$\eta(\alpha) = (1-\alpha)\frac{C_1\alpha}{C_1\alpha + 1} \tag{8}$$

that defines the mutual relationship for the interfacial heat transfer coefficients of the pseudo-liquid and the pseudo-gas for each value of the void fraction α (C_1 > 1.0 is a constant that defines the deformation of the shape function). The shape function is then multiplied by a large value C_2 to get the interfacial heat transfer coefficients

$$\begin{aligned} K_{\mathrm{ig}} &= C_2\eta(\alpha') \\ K_{\mathrm{il}} &= C_2\eta(1-\alpha') \end{aligned} \tag{9}$$

Finally, to prevent the phase change rate from dying-out too early as the void fraction approaches 0.0 or 1.0, the α' used in equation (9) is calculated from the pseudo void fraction α as

$$\alpha' = 0.5 - \frac{(\alpha - 0.5)^3}{0.25} \tag{10}$$

As stated above, the choice of K_{ig} and K_{il} is rather arbitrary, and the formulas presented here were derived through a process of trial and error – these definitions for the coefficients cause the void fraction to change from zero to unity (and vice versa) almost instantly in most situations where the bulk enthalpy enters the pseudo-two-phase region between $h_{\mathrm{l,sat}}$ and $h_{\mathrm{g,sat}}$.

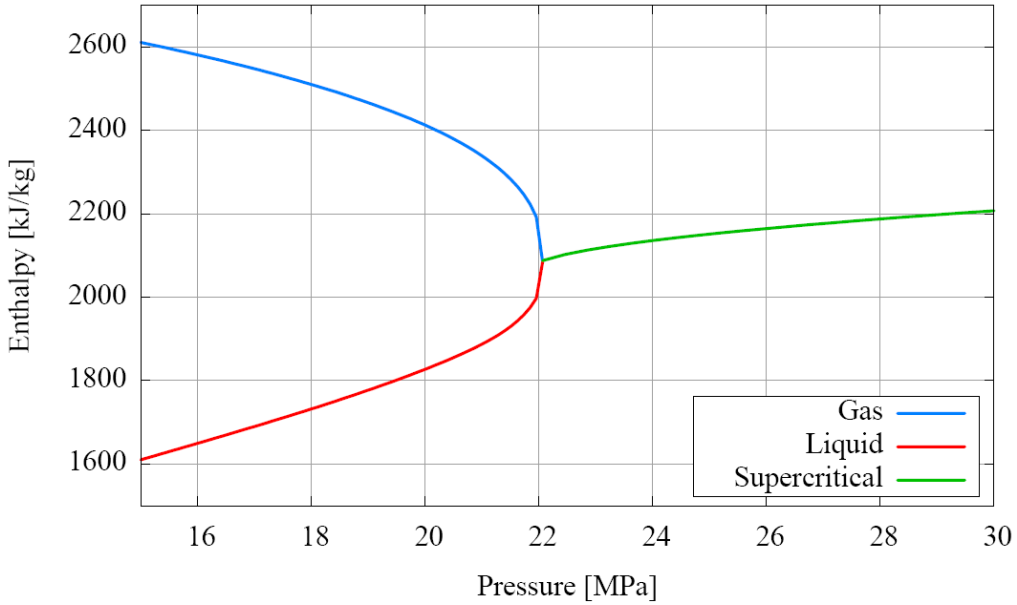

Fig. 1: Saturation enthalpies of gas and liquid. At supercritical pressures the saturation values are set to follow the pseudo-critical line.

2.3. Wall heat transfer

Above the critical pressure the boiling and condensation phenomena disappear and only one-phase convection occurs. Due to the possible pseudo two-phase conditions convection has to be calculated to both liquid and gas phases. However, to avoid the numerical problems during the transition over the critical pressure it is necessary to examine the heat transfer models of subcritical two-phase flow.

In two-phase region below supercritical pressure there are three basic separate heat transfer zones: wetted wall (zone 1), dry wall (zone 3) and a transition zone between wetted and dry wall (zone 2). The selection between different heat transfer zones is made on basis of wall and fluid temperatures, critical heat flux and minimum film boiling temperatures. In the wet wall area the two-phase heat transfer can be boiling or condensing. If the wall heat flux exceeds the critical heat flux the transition from the wet zone to dry zone occurs. If the wall temperature exceeds the minimum film boiling temperature the dry wall heat transfer is calculated.

In the following it is discussed how the wall heat transfer correlations behave near the critical pressure. Also it is described how the two-phase heat transfer mechanism must be modified at the supercritical pressure flow.

Total heat transfer of the nucleate boiling is calculated as a sum of the forced convection heat transfer to liquid and the nucleate boiling heat transfer. Because the evaporation heat does not exist at the supercritical pressure the boiling part of the heat transfer has to be fainted out. In two-phase area the nucleate boiling heat transfer is calculated with the Thom correlation [7]

$$h_{nb} = 1971.2\, e^{2p/8687000} \left(T_w - T_{sat}\right) \qquad (11)$$

In approaching the supercritical pressure the nucleate boiling term is multiplied with the ratio of evaporation heat to the enthalpy difference of smoothing area.

$$h_{cr} = r^n h_{nb} \tag{12}$$

$$r = \min\left[\frac{h(p_{cr}) - h(p)}{\Delta h}, 1.0\right] \tag{13}$$

Where $\Delta h = h(p_{cr}) - h(p_{sm})$ and p_{sm} is the lower limit for the pressure of smoothing area. In the two-phase area the heat flow from the nucleate boiling is divided to the heat flow to the liquid and to the heat flow to the interface q_{wi}, which is used in Equation (4). When the boiling heat transfer is fainted out the one-phase convection is a remaining mode.

In case of condensation it is assumed that steam condenses to liquid film on the wall (film condensation) and the heat transfer from liquid to wall is readily calculated with one-phase convection correlation. Therefore no special treatment in wall heat transfer due to condensation heat transfer is needed during the transition from subcritical to supercritical pressure.

In case of the dry wall it is assumed that the steam is in contact with the wall. This means that the one-phase heat transfer to steam is calculated already at subcritical pressure area. In that case the transition is easy if the same forced convection correlation can be used below and above the critical point.

When the pressure approaches the critical pressure the critical heat flux disappears. The disappearance of the critical heat flux brings about that the dry wall heat transfer is prevailing with positive heat flux (from wall to fluid). The wet zone heat transfer is calculated when the real heat flux is negative. Near the critical pressure the minimum film boiling temperature approaches the saturation temperature as can be seen in Equation (14), where the minimum film boiling temperature is calculated with the Groeneveld - Stewart correlation [7].

$$T_{MFB} = \left[T_{MFB}\left(9\cdot 10^6 Pa\right) - T_{sat}\left(9\cdot 10^6 Pa\right)\right]\frac{p_{cr} - p}{p_{cr} - 9\cdot 10^6} + T_{sat}, if\ p > 9\cdot 10^6 Pa \tag{14}$$

The different heat transfer zones have been defined in the following way. The wet wall zone is used when

$$T_W < T_{sat}$$

The dry wall zone is used when

$$T_{wall} > T_{mfs}$$

At the critical pressure point as indicated above

$$T_{mfs} = T_{sat}$$

resulting in that the zone 2 ceases to exist at the supercritical pressure area, i.e. only the heat transfer zones 1 or 3 are used. At the supercritical pressure condition it can be assumed that the heat transfer correlations are the same for pseudo liquid phase (zone 1) and in pseudo gas phase (zone 3). The zone 1 heat transfer is applied when the average enthalpy is less than pseudo saturation enthalpy, and the zone 3 heat transfer is calculated when the average enthalpy is above the pseudo saturation enthalpy.

Above the critical pressure point the heat transfer from wall to both pseudo liquid and pseudo gas is calculated with the correlation of Jackson and Hall [5]. The exponent n depends on the ratios of bulk, wall and pseudo critical temperatures. The correlation gives good values for the supercritical pressure heat transfer, but it does not predict the deterioration of heat transfer.

$$\mathrm{Nu_b} = 0.0183\,\mathrm{Re_b^{0.82}}\,\mathrm{Pr_b^{0.5}}\left(\frac{\rho_\mathrm{w}}{\rho_\mathrm{b}}\right)^{0.3}\left(\frac{\overline{c_p}}{c_{p,\mathrm{b}}}\right)^{n}$$

$$n = \begin{cases} 0.4, & \text{if } T_\mathrm{b} < T_\mathrm{w} < T_\mathrm{pc} \quad \text{or} \quad 1.2T_\mathrm{pc} < T_\mathrm{b} < T_\mathrm{w} \\ 0.4 + 0.2\left(\dfrac{T_\mathrm{w}}{T_\mathrm{pc}} - 1\right), & \text{if } T_\mathrm{b} < T_\mathrm{pc} < T_\mathrm{w} \\ 0.4 + 0.2\left(\dfrac{T_\mathrm{w}}{T_\mathrm{pc}} - 1\right)\left(1 - 5\left(\dfrac{T_\mathrm{b}}{T_\mathrm{pc}} - 1\right)\right), & \text{if } T_\mathrm{pc} < T_\mathrm{b} < 1.2T_\mathrm{pc} \quad \text{and} \quad T_\mathrm{b} < T_\mathrm{w} \end{cases} \tag{15}$$

2.4. Interfacial friction

Because above the critical pressure the distinction between gas and liquid does not exist, a good assumption to velocities of pseudo gas and liquid is that they flow with nearly the same velocity.

In the two-phase flow at subcritical pressure the interfacial friction is strongly dependent on the flow regime that is prevailing in the flow and the velocities of phases may largely differ from each other. The largest velocity difference is related to stratified flow. Different interfacial friction correlations are used for the different flow regimes. The modeled flow regimes are stratified flow and non-stratified flow consisting of bubbly, annular and droplet flow. The final value for the interfacial friction is then obtained as a weighted average of the different correlations. Void fraction, rate of stratification and rate of entrainment are used as weighting coefficients. The final interfacial friction is calculated using interfacial friction of different flow regimes and the weighing factors for stratification and entrainment (Equation 16).

$$F_i = RF_{is} + (1-R)\{(1-E)[(1-\alpha)F_{ib} + \alpha F_{ia}] + EF_{id}\} \tag{16}$$

In the definition of the rate of stratification the general form of the Kelvin-Helmholtz stability criterion is used (see Equation 17).

Because the liquid and steam densities approach each other at the supercritical pressure the stratification disappears, i.e. the stratification rate R approaches zero.

$$\left(u_g - u_l\right)^2 < gD\left(\rho_l - \rho_g\right)\left(\frac{\alpha}{\rho_g} + \frac{1-\alpha}{\rho_l}\right) \tag{17}$$

Because the surface tension disappears at the critical pressure the entrainment weighing factor approaches to 1 providing that the pseudo void fraction is not zero.

$$E = \left(1 - \frac{1.8 \cdot 10^{-4} \cdot \sigma}{\alpha \left|u_g\right| \eta_g} \sqrt{\frac{\rho_l}{\rho_g}}\right)^2 \cdot f(\alpha) \tag{18}$$

Because near the critical pressure the stratification disappears and droplet flow is prevailing flow regime the interfacial friction inherently becomes large in approaching the critical pressure.
At the critical pressure it is required that the pseudo liquid and gas flows nearly with the same velocity. Therefore for the interfacial friction a large number is used. In order to avoid instabilities the linear interpolation between the subcritical interface coefficient and the large supercritical coefficient is performed over the pressure interval around the critical pressure.

2.5. Wall Friction

The friction between one phase (liquid or gas) and the wall of the flow channel is calculated with the formula

$$F_{wk} = -\frac{1}{2} \frac{f_k \rho_k u_k \left|u_k\right|}{D_H} \tag{19}$$

The quantity f_k is the friction pressure loss coefficient or friction factor for phase k. The used friction factors of phases consist of the single phase friction factor and the two phase friction multiplier:

$$f_k = f_{sp,k} \cdot c_k \tag{20}$$

The purpose of the two phase friction multiplier is to expand the pressure drop calculation of single phase flow and to estimate the phase distribution on the wall of the flow channel. The multiplier is defined separately for the following flow regimes: stratified flow, non-stratified flow without droplet entrainment and non-stratified flow with droplet entrainment. The rate of stratification and rate of entrainment are used as weighting coefficients when the multiplier is calculated.

$$c_g = R \cdot c_{g,st} + (1-R)\, c_{g,ns} \tag{21}$$

$$c_l = R \cdot c_{l,st} + (1-R)\left\{(1-E)c_{l,ne} + E \cdot c_{l,en}\right\} \tag{22}$$

In case of the supercritical pressure the stratification becomes zero and the entrainment approaches one and therefore in the calculations of the multipliers the non-stratified part is used for the gas and the entrainment part is used for the liquid.

$$c_g = c_{g,ns} = \alpha^{1.25} \tag{23}$$

$$c_l = c_{l,en} = \frac{(1-\alpha)\rho_l}{\alpha\rho_g + (1-\alpha)\rho_l} \tag{24}$$

In Equations 23 and 24 it can be seen that the wall friction is mainly calculated for liquid only when void fraction approaches 0 and when the void fraction is near 1 the wall friction multiplier to gas becomes predominant.

At the subcritical area the single phase friction factors are calculated either with Blasius equation (smooth pipes) or with the Colebrook equation, which takes into account the roughness of pipes.

In the supercritical pressure region the correlation of Kirillov *et al.* [3] is recommended:

$$f_{sp,k} = \frac{1}{\left(1.82\log_{10}(\mathrm{Re_b}) - 1.64\right)^2}\left(\frac{\rho_\mathrm{w}}{\rho_\mathrm{b}}\right)^{0.4} \tag{25}$$

The friction factor f_k is calculated for both pseudo liquid and pseudo gas. The phase friction multipliers from Equations 23 and 24 are then used to calculate the phase friction factors that are finally used for the wall friction calculation.

3. TESTING OF THE MODEL

3.1. Testing of the transition from supercritical to subcritical pressures

Ability of the numerical model to calculate transition from the supercritical pressure region to the subcritical pressure region was tested by calculating an imaginary experiment, in which a closed pipe initially filled with water at a supercritical pressure was nearly instantaneously emptied. This simulated experiment is identical to the Edwards-O'Brien blowdown test [6], except for the initial pressure which was about 7 MPa in the original real-life experiment. Because this test is purely imaginary, experimental data is not available, and thus no definitive conclusions can be drawn on the validity of the model based on the simulation results. Thus, the simulation serves only to demonstrate that the numerical model is able to simulate the transient.

In the simulated experiment a straight horizontal pipe of 4.096 m length and 73 mm inner diameter is initially closed and filled with water at state p_0, T_0. Then an orifice with cross-sectional area of 87 % from the pipe's cross-sectional area is opened at one end of the pipe in an interval of 10 ms. The opening of the orifice causes a depressurization wave to travel through the pipe, which in turn causes the liquid in pipe to flash. Expansion of the fluid in the pipe makes it flow out of the pipe with a very large velocity, which is, however, limited by the critical velocity at the break orifice.

This experiment was simulated several times with different initial temperatures T_0, to ensure that the numerical model can cope with passing through the critical point (22.064 MPa, 373.946 °C) in which the thermophysical property changes are the steepest. The initial temperatures are listed in table 1, the initial pressure was 25.0 MPa for all tests.

Table 1: Initial temperatures of the blowdown simulations

	Test 01	Test 02	Test 03	Test 04	Test 05	Test 06	Test 07
T_0 [°C]	300.0	374.0	377.0	380.0	383.0	386.0	500.0

Time-behavior of pressure and void fraction during three of these simulations is presented in figure 2. In test 01 pressure drops in the whole pipe very quickly due to the high velocity of sound at the initial state ($c_0 \approx 1039$ m/s). The local minimum observed at the closed end at about 0.004 s is caused by reflection of the depressurization wave, and it's occurrence in time is in excellent agreement with the time the depressurization wave should travel the pipe (4.096 m / 1039 m/s ≈ 0.0039 s). Later ridges in the plot are caused by the pressure wave traveling back and forth in the pipe with its velocity altered by lowering enthalpy of the fluid, and evaporation.

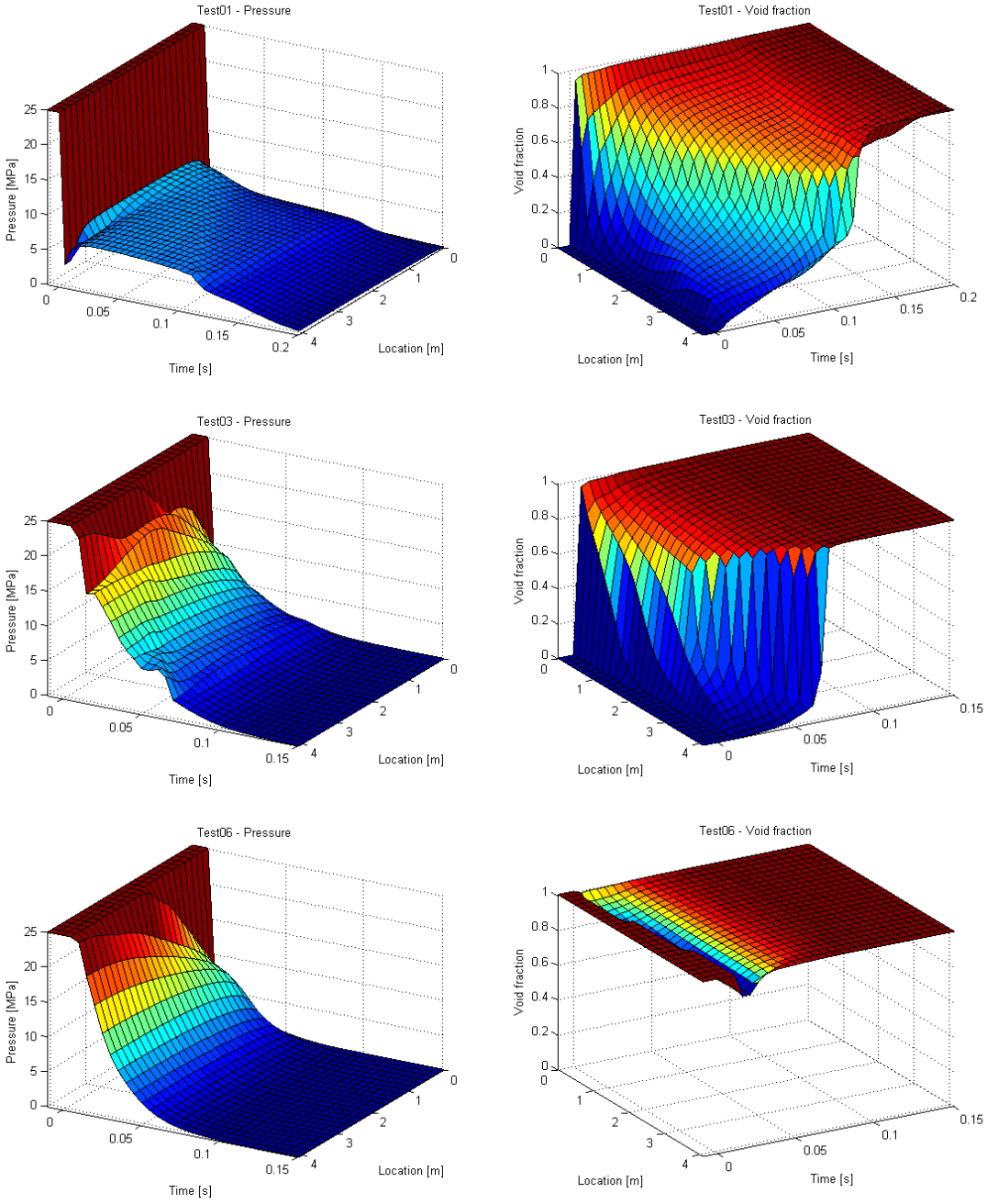

Fig. 2: Behavior of pressure and void fraction during the blowdown tests 01, 03 and 06. Location is the distance from the break orifice. Notice also the different view angles in the pressure and void fraction graphs.

Test 03 is similar to test 01, but the sonic velocity in the initial state is very low due to the initial temperature which is near the pseudo-critical temperature ($c_0 \approx 477$ m/s). This manifests itself as slower depressurization of the closed end.

Finally in test 06, the pipe contains initially (pseudo-)gas and thus the depressurization is still slow ($c_0 \approx 731$ m/s), but the flashing doesn't happen. However, in this case enthalpy of fluid drops below the steam saturation enthalpy and this causes some of the fluid to temporarily condensate.

As a conclusion of these simulations, it can be stated that APROS is capable of calculating this kind of a fast transition from supercritical to subcritical pressures, and the results seem at least quantitatively correct. However, real-life test data is still needed to validate the code.

3.2. Testing of the pseudo-phase transition

The transition from pseudo-liquid state to pseudo-gas phase and back was tested by simulating flow through a thin heated pipe in which the pseudo-critical state was passed. The diameter of the vertical pipe (4 mm) corresponded to a typical hydraulic diameter of the flow channels in a planned supercritical water reactor (SCWR).

In the simulation a constant pseudo-liquid mass flow of 0.04 kg/ at 310 °C was let flow in the lower end of the pipe, and the upper end of the pipe was kept at constant pressure of 25.0 MPa. The pipe was heated with 50 kW of power between times 1.0 s and 10.0 s. This power was enough to raise the outlet temperature above the pseudo-critical temperature (384 °C at 25.0 MPa), up to 405 °C. The pipe was divided to 20 internal nodes, and the wall-to-fluid heat transfer was calculated with the correlation of Jackson and Hall.

Development of temperature and void fraction distributions in the pipe are presented in figure 3. As can be readily seen, the void fraction changes between zero and unity almost instantly when the pseudo-critical temperature is passed. In the first node in which the pseudo-critical temperature is passed, the void fraction changes only to about 90 %, but in the next node the void fraction is already at about 99 %. This happens because the superheating of the pseudo-liquid phase is not sufficient to evaporate the whole mass contents of the node in this case. Subsequent simulations with varied heat flows and node volumes revealed similar development for the void fraction distribution.

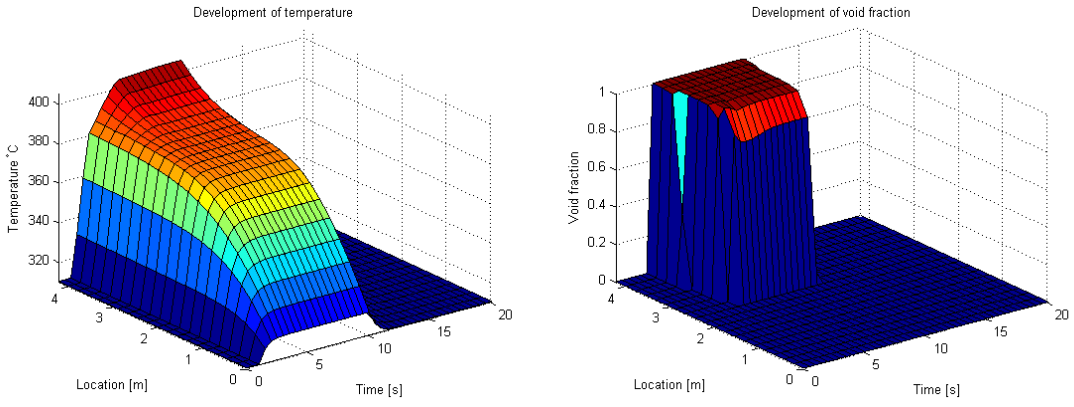

Fig. 3: Development of temperature and void fraction during the pseudo-phase transition test.

Although the pseudo-phase transition is not fully optimal (i.e. the void fraction does not change between zero and unity in a single time step), it can be still considered very satisfactory, as the (pseudo-)void fraction is insignificant as long as the pressure stays above the critical point. The pseudo-void fraction distribution can have effect on any real (measurable) variables only when simulating situations where the pressure is allowed to drop below the critical point. Because such transitions happen typically very

fast, and because many other phenomena are involved in the transition, it is the present authors' belief that the effect of the void fraction distribution is insignificant even in these kinds of simulations. However, experimental data is needed to verify this argument.

4. CONCLUSION

The most important changes implemented into APROS thermal hydraulic system code, in order to make it work at the supercritical pressures region, have been presented. The behavior of constitutive equations in two-phase flow at the transition from subcritical pressure to supercritical pressure has been described. The ability of the new models has been demonstrated by calculating two basic transients. The simulations with various initial states and boundary conditions prove that the transition from subcritical to supercritical conditions takes place in a sound manner without numerical problems. Also at supercritical pressure the transition from pseudo liquid to pseudo gas due to heat transfer takes place fast and without any numerical problems. In order to closer examine the accuracy of model experimental data is needed.

ACKNOWLEDGMENTS

The authors appreciate to Fortum Nuclear Services Ltd for funding this work together with VTT Technical Research Centre of Finland.

Nomenclature

C	constant
c	specific heat capacity, speed of sound
E	rate of entrainment
F	force
g	gravitational acceleration
h	total specific enthalpy (i.e. including kinetic energy)
K	heat transfer coefficient
$\mathcal{L}$	evaporation heat
Nu	Nusselt number
p	pressure
Pr	Prandtl number
q	heat transfer rate
R	rate of stratification
Re	Reynolds number
t	time
T	temperature
u	velocity
z	location
α	void fraction (volume fraction of the gas phase)
Γ	mass transfer rate
θ	inclination
μ	dynamic (absolute) viscosity
ν	kinematic viscosity
ρ	density
σ	surface tension
τ	friction

Subscripts

b	bulk
g	gas
h	hydraulic

i	interface
k	phase *k* (l or g)
l	liquid
pc	pseudo-critical
pe	pseudo-evaporation
sat	saturation
stat	static (without kinetic energy)
w	wall

REFERENCES

1. J. Kurki, “Simulation of thermal hydraulics at supercritical pressures with APROS”, Thesis for the degree of Master of Science in Technology, Helsinki University of Technology, Department of Engineering Physics and Mathematics, 2008.
2. T. Siikonen, “Numerical Method for One-Dimensional Two-Phase Flow”, Numerical Heat Transfer, **12**, 1—18, 1987.
3. I. Pioro, R. Duffey and T. Dumouchel, “Hydraulic resistance of fluid flowing in channels at supercritical pressures (survey)”, Nuclear Engineering and Design, **231**, 187—197, 2004.
4. I. Pioro, H. Khartabil and R. Duffey, “Heat transfer to supercritical fluids flowing in channels – empirical correlations (survey)”, Nuclear Engineering and Design, **230**, 69—91, 2004.
5. J. D. Jackson and W. B. Hall, “Forced convection Heat Transfer to Fluids at Supercritical Pressure”, in “Turbulent Forced Convection in Channels and Bundles”, **2**, edited by S. Kakaç and D. B. Spalding, Hemisphere, 1979.
6. A. R. Edwards and T. P. O’Brien, “Studies of phenomena connected with the depressurization of water reactors”, Journal of British Nuclear Energy Society, **9**, 125—135, 1970.
7. D. C. Groeneveld and C. W. Snoek, “A Comprehensive Examination of Heat Transfer Correlations Suitable for Reactor Safety Analysis”, Multiphase Science and Technology, **2**, 181—274, 1986.